Appendix B: Estimation of Losses due to rain at 10 GHz

The potential for attenuation due to rainfall was examined retrospectively for two purposes. First, we wanted to estimate rainfall attenuation losses that might have been present and thus have contributed to signal attenuation along the RF path on 10 GHz at the time we received our strongest 432 MHz signals across the duct between CA and HI, between 2200Z and 2300Z on July 15, 2022. Second, we wanted to assess the likely magnitude of rainfall attenuation losses that might be experienced by future propagation attempts on 10 GHz across this path.

Attenuation due to rainfall is discussed in ITU-R P.837-7, "Characteristics of precipitation for propagation modeling"[i] and ITU-R P.838-3, "Specific attenuation model for rain for use in prediction methods"[ii]. These documents provide an excellent reference on this topic. In addition, a recent extensive review by Alozie et al of rainfall attenuation is an excellent introduction to this topic[iii] and provides numerous references.

In this project we used the method for calculating rainfall attenuation described in the ITU document P.838-3 in which the authors calculate the specific attenuation due to rain using these equations:

$\gamma_R = kR^\alpha$ where γ_R is the specific attenuation due to rainfall in dB/km, R is the rain rate in mm/h,

and α and k are determined as functions of the frequency f (in GHz) from the following equations given in ITU-R P.838-3:

$$\log_{10} k = \sum_{j=1}^{4} \left(a_j \exp\left[-\left(\frac{\log_{10} f - b_j}{c_j} \right)^2 \right] \right) + m_k \log_{10} f + c_k \qquad (2)$$

$$\alpha = \sum_{j=1}^{5} \left(a_j \exp\left[-\left(\frac{\log_{10} f - b_j}{c_j} \right)^2 \right] \right) + m_\alpha \log_{10} f + c_\alpha \qquad (3)$$

where:

f: frequency (GHz)

k: either k_H or k_V

α: either α_H or α_V.

Table look-ups for the coefficients on the right-hand side of equations 2 and 3 above for k and α respectively are required in order to perform these calculations and this in practice adds complexity to these calculations.

Fortunately, MATLAB has an implementation of this method (rainpl[iv]) that simplifies the calculation process. Rainfall attenuation can also be calculated without the need to resort to table lookups by using the software package MPM93[v,vi] which is an update of MPM87 by Liebe and Layton[vii].

For this project we chose to use the rainpl function in MATLAB because of its ease of use for evaluating large data sets as well as because it was based on the ITU method which is an accepted, widely used standard method for this task. The software package R[viii] was used for performing some subgroup analyses when those analyses were more conveniently performed in R than in MATLAB.

We used 3 libraries of satellite rainfall data in our analysis. With each of these we used NASA's Panoply software to get a broad, rapid imaging-based overview of the rainfall across the Pacific Ocean between our CA and HI locations for the time frame being examined. We then used numerical non-imaging-based analysis to examine the details of rainfall on the path, using data from the same data sets. The 3 data sources provided us with a range of temporal granularity. The finest granularity was provided by the IMERG (Integrated Multi-satellitE Retrievals for GPM)[ix] 3B-HHR-L.MS.MRG.3IMERG data set which gave 30-minute-time-resolution data sets. 10-hour blended data sets from the NESDIS Operational Blended Rain Rate Product[x] containing data from 8 polar-orbiting satellites (POES NOAA-19, NOAA-20, MetOp-B, S-NPP, GCOM-W1, GPM, DMSP F17 and F18) supplied intermediate time-resolution data via the BHP-RR_v01r1_blend library, and the Suomi NPP[xi] 3A-CLIM-DAY.NPP.ATMS.GRID[xii][xiii] library gave 24-hour resolution data sets. The Suomi NPP ATMS (Advanced Technology Microwave Sounder)[xiv] is able to penetrate cloud cover and it provides accurate satellite-based measurements of precipitation rates including the rainfall rates which we required. The IMERG data set is a multi-satellite dataset using the GPM satellite constellation[xv] that provides precipitation estimates using both microwave-based and IR-based sensors.

For the numerical analysis that we performed after our initial imaging-based evaluation, we limited the data set to points within 0.1 degrees of the RF path in order to avoid contaminating the quantitative results along the RF path with data from extraneous locations not along the path. The map below shows in red the width and path of the extracted 0.1 degree satellite data sets that we used for numerical analysis.

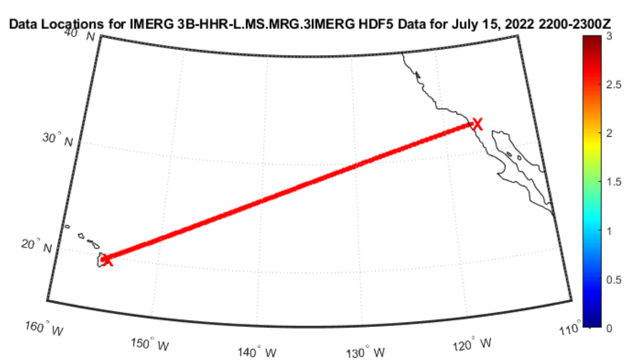

Figure 1. Map showing extent of data set used for numerical analysis, in red.

The image below is taken from the 3B-HHR-L.MS.MRG.3IMERG data set for the 30 minute time window when we had our strongest signals on 432 MHz on July 15, at 2200-2230Z It shows the Pacific Ocean in the region of our RF path with San Diego near the right edge of the map and Hawaii near the left edge. In this view you can see, if not on the image in this pdf file, then on the linked image on the web, a very small area of rain along the path just east of the island of Hawaii:

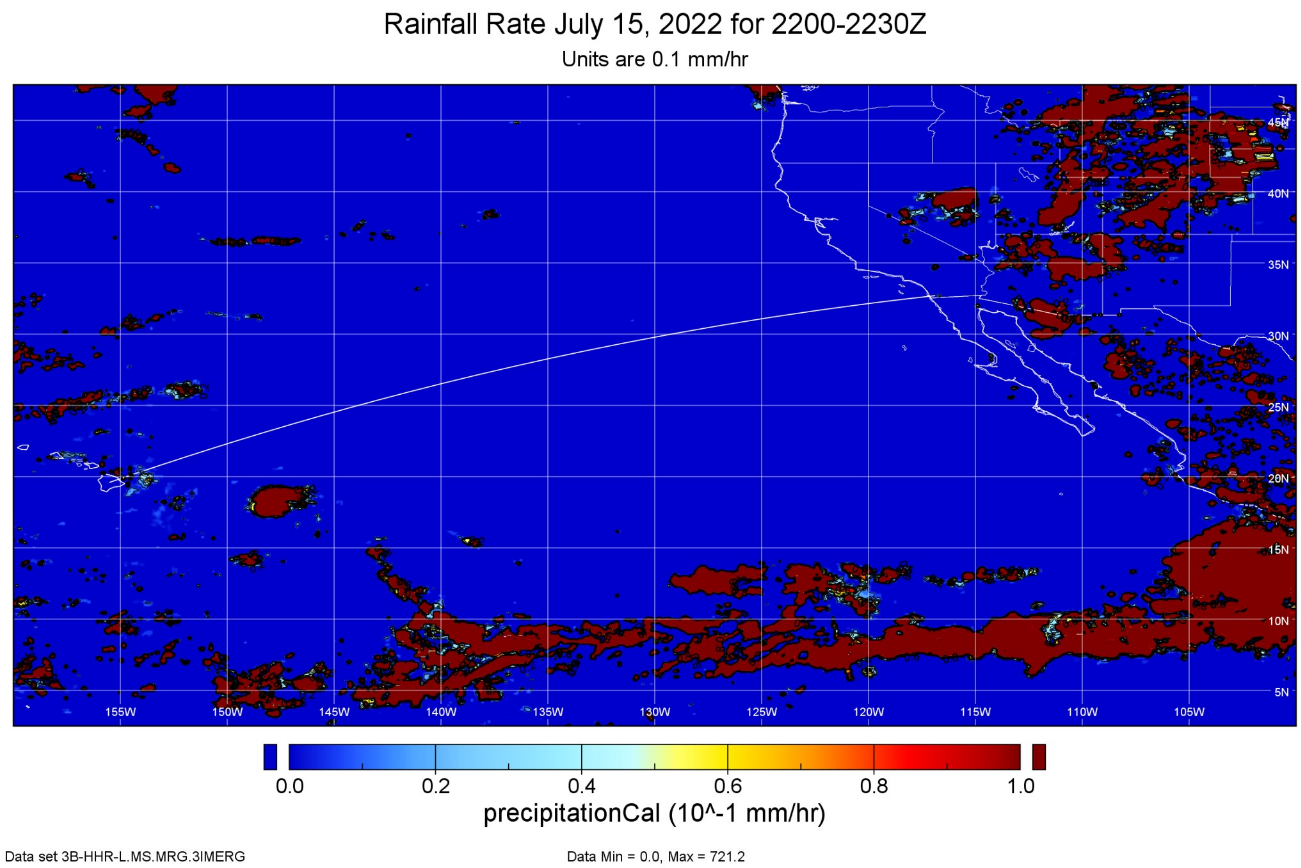

Figure 2. IMERG data for July 15, 2022 2200-2230Z displayed using NASA's Panoply software. Maximum color shown at rain rate of 0.1 mm/hr. This image is also available here.

On this map we set the maximum color scale bin for a rain rate of only 0.1 mm/hr in order to accentuate very small amounts of rain that would not otherwise be visible.

Because the best reception of 432 MHZ signals from CA at our HI location occurred at 2228 Z on July 15, for our numerical analysis we used the 30-minute resolution IMERG data to examine the time interval from 2200-2300Z on July 15 along and within 0.1 degrees of the great circle RF path between our two locations. This analysis showed that the maximum precipitation rate on or near our path during the indicated time interval was only 0.283 mm/hr, occurring as seen above in only a small area off the east coast of Hawaii.

The graph below derived from this data shows rainfall rates over the entire CA-HI path for 2230-2300 on July 15, 2022 for data points that are within 0.1 degrees of the great circle path between San Diego and our Mauna Loa Observatory Road Site #3.

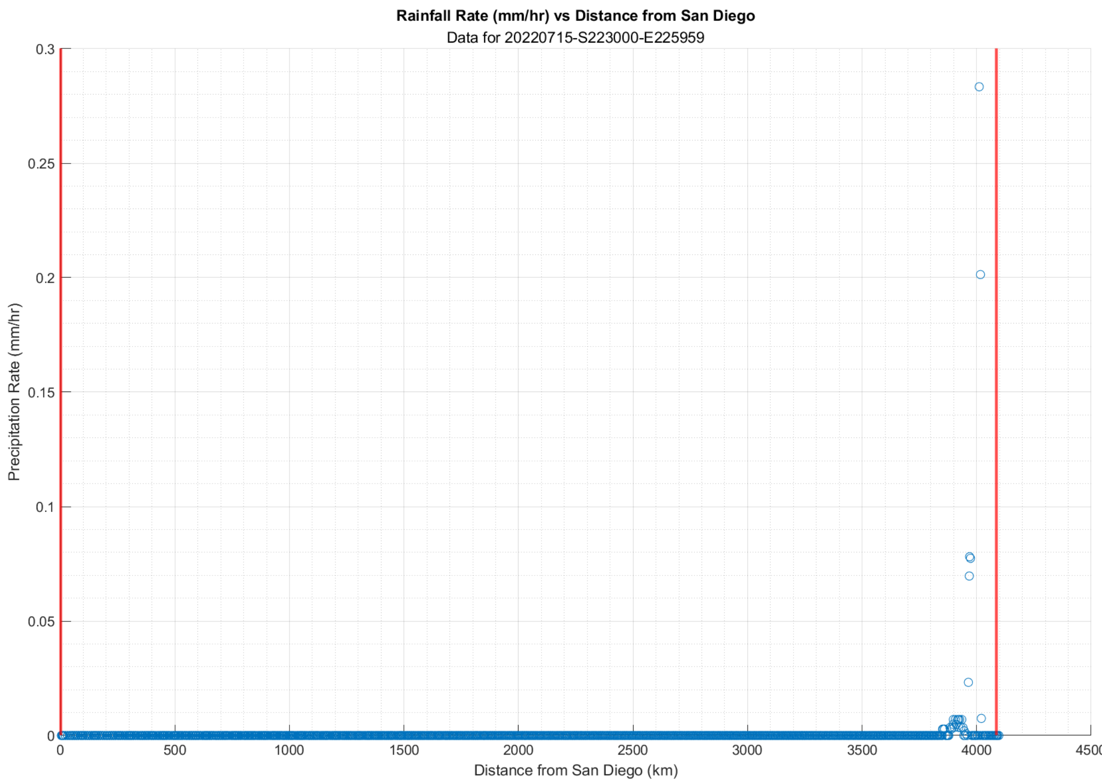

Figure 3. Rainfall rate taken from IMERG data for 2230-2300 Z July 15 for points within 0.1 degree of great circle RF path between our CA and HI locations. This figure is also available here.

Although you can see on this graph that the maximum precipitation rate of 0.283 mm/hr occurs less than 100 km east of our HI location which is marked by a red vertical line at 4086 km, this is much more easily seen on the following graph, which shows only distances from 3700 to 4100 km along the path:

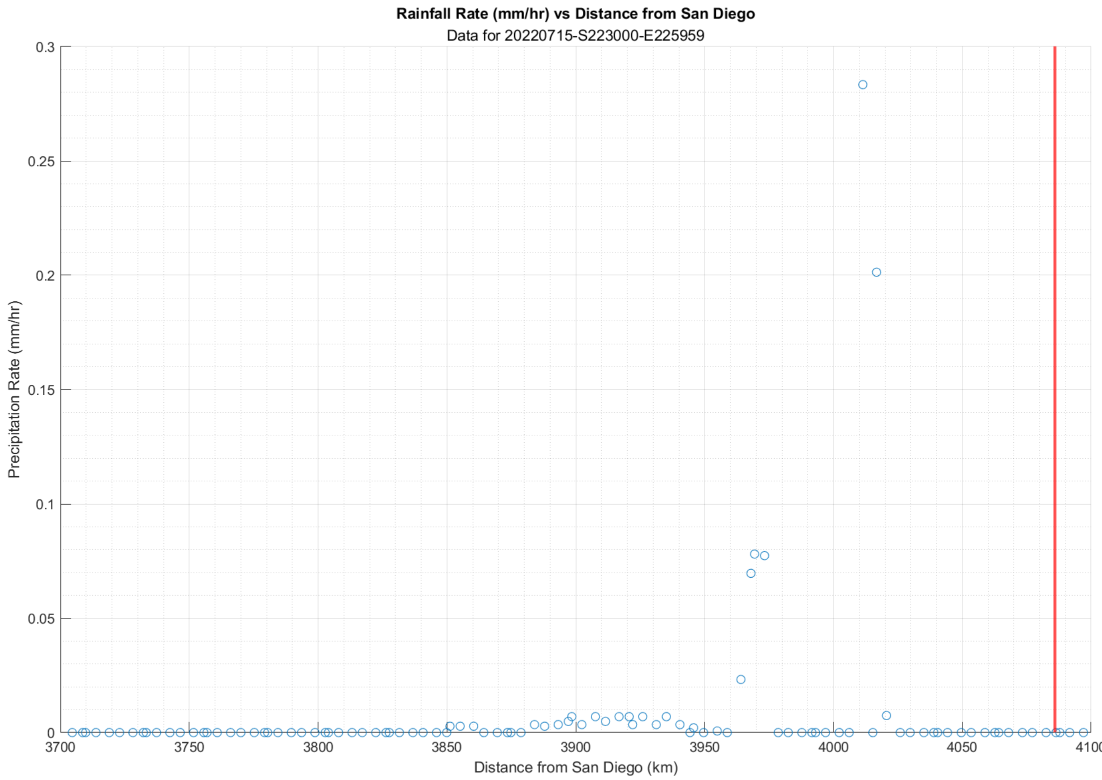

Figure 4. Zoomed graph of rainfall rate taken from IMERG data for 2230-2300 Z July 15 for points within 0.1 degree of great circle RF path between our CA and HI locations. This figure is also available here.

Although some rain does extend eastward from the location of peak rainfall at approximately 4012 km, the rain rate is greater than 0.3 mm/hr for only one data point, representing a distance of less than 5 km. The rain rate is greater than 0.2 mm/hr over a distance of well less than 10 km and beyond that distance the rain rate is on the order of 0.1 mm/hr or less, falling to negligible amounts east of 3960 km.

The results of calculating the rainfall attenuation coefficient for each data point are shown in the next graph below, which is also zoomed for clarity to show just 3700-4100 km. You can see that the peak rainfall attenuation coefficient, at ~4012 km, approximately 75 km east of our HI operating site, is 0.0074 dB/km. Although this would represent an attenuation of 30 dB if this amount of rain extended across the entire path, because the rainfall is localized to such a small segment of the path, the mean rainfall attenuation coefficient for the entire path is 1.73e-05 dB/km, so that the estimated total rainfall attenuation across the entire 4086 km path is only 0.07 dB.

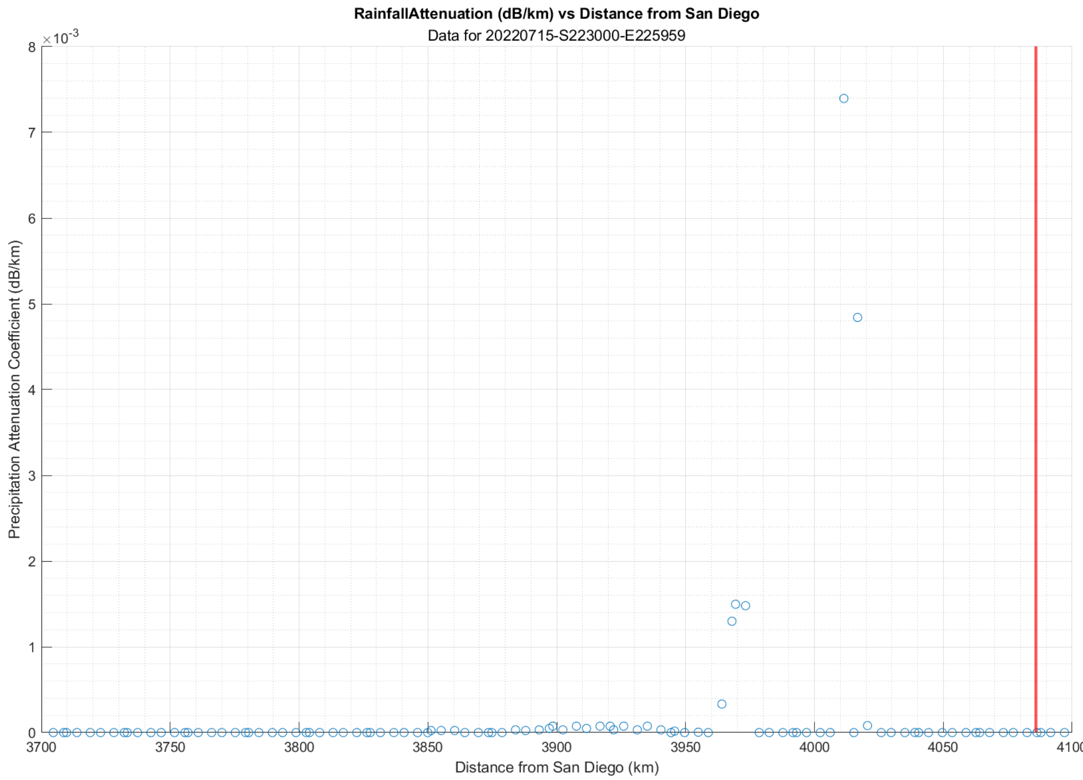

Figure 5. Rainfall attenuation coefficient taken from IMERG data for 2230-2300 Z July 15 for points within 0.1 degree of great circle RF path between our CA and HI locations. This figure is also available here.

It turns out that these conditions were more favorable than was generally the case along the RF path during the month of July, 2022. Using the 24-hour resolution Suomi dataset to examine the entire 24-hour period on July 15, we found that the peak total rainfall attenuation across the path on July 15 was 1.9 dB, roughly 30 times what it was when we received our strongest signals.

Furthermore, it turns out that July 15 was not among the rainiest days during July. Examination of the rainfall data for the period from July 1-July 27, 2022 showed that the date with greatest rainfall rate was July 14, and on that date the total rainfall attenuation across the path was 3.7 dB. Daily total path rainfall attenuation for July 2022 is shown on the graph below:

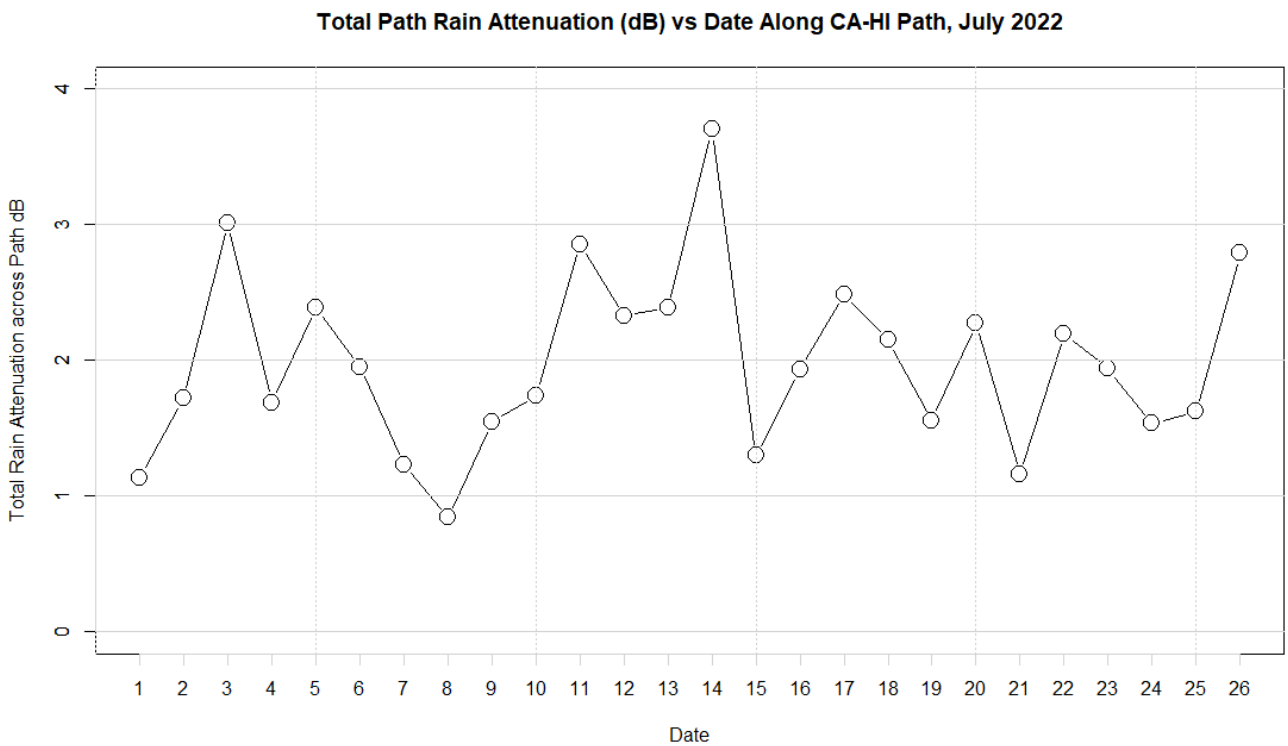

Figure 5. Total Rainfall Attenuation across the CA-HI Path for July, 2022. This figure is also available here.

Of course, even the largest values of total rain attenuation across the path that occurred during the month of July 2022 are orders of magnitude smaller than the total values for gaspl and LWC attenuation along the path that were detailed in Appendix A, so it is clear that rainfall attenuation was not responsible for our failure to communicate on 10 GHz across the path on July 15, 2022. And it is clear that for most periods rainfall attenuation will not be an important component of signal loss at 10 GHz along the path.

Summary

Although rain attenuation can be severe on 10 GHz, based on the above analysis it did not appear to be a significant issue during our operating periods while attempting to achieve communications on 10 GHz across the CA-HI duct during July, 2022.

The potential for attenuation due to rainfall along the RF path between our San Diego, CA and Hilo, HI operating sites was examined using data for July 2022 from the IMERGE and Suomi NPP satellite data sets and estimated rainfall attenuation during those times was consistently less than 4 dB, orders of magnitude less than the attenuation due to atmospheric gas, water vapor, and liquid water content.

--Roger Rehr W3SZ 2/19/2023

i ITU R-REC-P.837.7: ”Characteristics of precipitation for propagation modelling”, https://www.itu.int/dms_pubrec/itu-r/rec/p/R-REC-P.837-7-201706-I!!PDF-E.pdf, 2017.
ii ITU-R-REC P.838-4: “Specific attenuation model for rain for use in prediction methods”, https://www.itu.int/dms_pubrec/itu-r/rec/p/R-REC-P.838-3-200503-I!!PDF-E.pdf
iii Alozie E et al: “A Review on Rain Signal Attenuation Modeling, Analysis and Validation Techniques: Advances, Challenges and Future Direction”, Sustainability14: 11744, 2022. https://www.mdpi.com/2071-1050/14/18/11744
iv https://www.mathworks.com/help/phased/ref/rainpl.html
v https://its.ntia.gov/research-topics/radio-propagation-software/mpm/millimeter-wave-propagation-model-mpm/
vi MPM93 software may be downloaded from the NTIA website via this link: https://its.ntia.gov/media/35413/mpm93.zip
vii Liebe HJ, Layton DH. “Millimeter wave properties of the atmosphere”, NTIA Tech Report TR-87-224,1987. Available for download from NTIA website via this link: https://its.ntia.gov/umbraco/surface/download/publication?reportNumber=87-224.pdf
viii https://www.r-project.org/
ix https://gpm.nasa.gov/data/imerg
x https://www.avl.class.noaa.gov/saa/products/search?sub_id=0&datatype_family=BLENDHYDRO&submit.x=19&submit.y=3
xi https://www.avl.class.noaa.gov/release/data_available/npp/index.htm
xii https://storm.pps.eosdis.nasa.gov/storm/
xiii https://storm.pps.eosdis.nasa.gov/storm/data/Service.jsp?serviceName=Order
xiv https://www.nesdis.noaa.gov/current-satellite-missions/currently-flying/joint-polar-satellite-system/advanced-technology
xv https://gpm.nasa.gov/missions/GPM/constellation